DETACHED BREAKWATERS

TORU SAWARAGI

Professor, Department of Civil Engineering
Osaka University
Yamada-oka, 2-1, Suita-city, Osaka 565, JAPAN

1. FUNCTION OF DETACHED BREAKWATER IN CONTROLLING WAVES AND WAVE-INDUCED CURRENTS

1.1. Historical background and present situation of shore protection works in Japan

Japan is surrounded by sea with a total 34360 kilometers of shoreline. 47% of the shoreline, or 15991 km, requires protection works to avert potential disasters.

Since World War II Japan has depended heavily upon hydraulic power for its electricity. A large number of hydroelectric stations and dams were constructed, and the dams trapped a huge amount of sediment, resulting in significant erosion of many coasts.

The Japanese Coastal Law was enacted in 1953 to regulate two kinds of engineering works that provide protection against coastal disasters. One group mitigates storm surges and the other beach erosion. Needless to say, there are also engineering works for coastal disasters caused by wave overtopping, tsunamis, blockage of river mouths and so on. Various kinds of coastal structures such as sea dikes, seawalls, lockgates, detached breakwaters, groins, artificial reefs, and wave absorbing block mounds have been constructed to provide protection against these disasters (see Table 1).

Table-1 Total length of shoreline with protection works (1988)

Structure	Sea walls	Sea dikes	Groins	Detached breakwaters	Wave absorbing blocks
Total length	2870 km	5960 km	367 km	630 km	1100 km

Figure 1 illustrates the ratio of increase of the region where these kinds of coastal structures were constructed, using 1962 as a base year (Toyoshima, 1986).

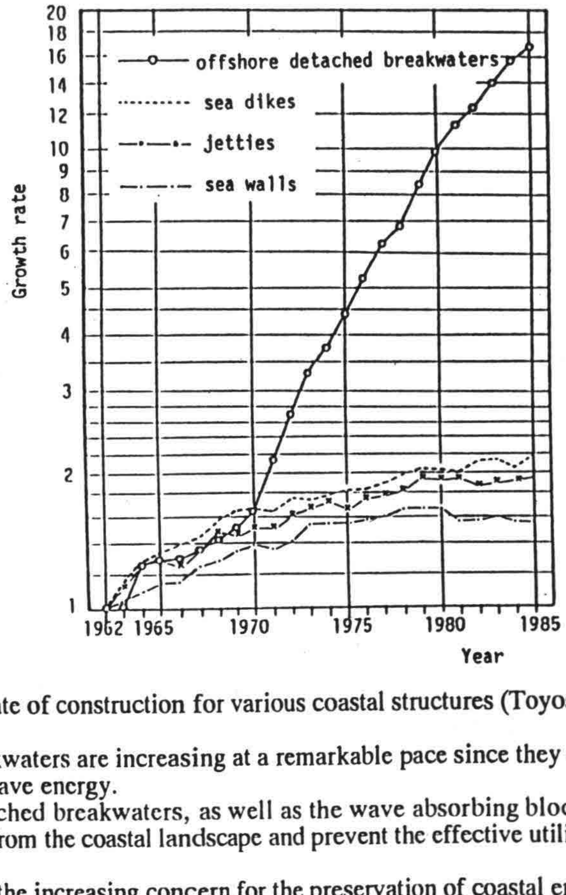

Fig.1 Rate of construction for various coastal structures (Toyoshima, 1986)

Detached breakwaters are increasing at a remarkable pace since they effectively reduce and absorb incident wave energy.

However, detached breakwaters, as well as the wave absorbing block mounds in front of seawalls, detract from the coastal landscape and prevent the effective utilization of many coastal regions.

Recently, with the increasing concern for the preservation of coastal environments and easier access to the shoreline, and with demands for pro-water front, new forms of coastal protection works have been devised in Japan:

1) gentle slope sea dikes with permeable surfaces,
2) submerged breakwater with wide crown widths or artificial reef,
3) beach nourishment,
4) head-land defense works.

In this paper, the hydraulic functions and stability of detached breakwaters and submerged breakwaters with wide crown widths are discussed.

1.2. Function of detached breakwaters in the control of waves

Two wave forms are found behind detached breakwaters: waves transmitted the breakwater and waves diffracted from the two ends of the breakwater. Wave height behind the breakwater is often estimated from the energetic mean of these two kinds of waves. In Japan, the wave height behind the group of detached breakwaters (H) is usually estimated by the following equation (National Association of Sea Coast, 1987):

$$\frac{H}{H_i} = \sqrt{\frac{l}{l+l'} K_t^2 + \frac{l'}{l+l'} K_g^2} \tag{1}$$

where l is the length of the detached breakwater, l' is the length of the opening in the row of detached breakwaters, K_t is the transmission coefficient through the breakwater, and K_g is the diffraction coefficient at openings in the breakwaters (see Fig.2).

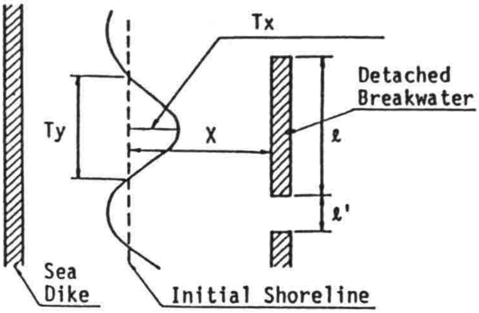

Fig.2 Definition sketch of a plane arrangement of detached breakwaters

Various studies have been conducted to determine the value of K_t, the transmission coefficient. The following is the empirical expression for K_t derived by Numata (1975) under conditions where wave overtopping takes place:

$$K_t = 0.123 \log\left(43.12 \frac{u_{max}\eta_c T}{B h_s}\right) \tag{2}$$

where B is the breakwater width at still water level, h_s is the crown height from still water level, η_c is the height of wave crest from still water level. The expression u_{max} represents maximum water particle velocity at the wave crest and is expressed as:

$$u_{max} = \frac{\pi H_i}{T} \sqrt{1 + m_1 \left(\frac{H_i}{h_o}\right)^{0.5} \left(\frac{h+\eta_c}{h_o}\right)^3 \frac{\cosh k(h_o+\eta_c)}{\sinh k h_o}} \tag{3}$$

$$\begin{aligned} m_1 &= -0.644 \log\{1.562(h_o/L)\} &&: 0.07 < h_o/L < 0.4 \\ &= 1.50 &&: h_o/L < 0.07 \\ &= 0.25 &&: 0.4 < h_o/L \end{aligned}$$

where h_o is water depth where the breakwater is constructed, L is the wave length at depth h and $k=2\pi/L$. Numata also gave the relation between η_c/h_o and H_i/h_o as follows:

$$\frac{\eta_c}{h_o} = \frac{H_i}{2h_o} + 0.415\left(\frac{H_i}{h_o}\right)^{2.18} \tag{4}$$

Although the exact value for K_g has to be calculated from the diffraction pattern, values of between 0.7 and 0.9 are usually substituted in actual calculations of Eq.(1).

In Eq.(1) the effect of interaction between waves and structures is not taken into account. Recently, a boundary integral method has been developed to solve a wave field around structures such as detached breakwaters in which the effect of wave-structure interaction is fully considered. For example, Spring (1975) has solved the wave field resulting from a regularly spaced infinite row of vertical cylinders, and Pullin (1984) has developed a numerical procedure for solving waves around a group of vertical structures. In these procedures, wave fields around structures are calculated by solving velocity potential as a boundary value problem.

The velocity potential around structures ϕ is expressed as the sum of the velocity potential of incident waves ϕ_i and a scattered wave potential ϕ_s, $\phi=\phi_i+\phi_s$. The unknown potential ϕ_s is usually evaluated by a finite element method or a boundary element method. Compared with the former method, the latter requires less computer capacity and CPU time because variables in the latter method are one order lower in dimension than those in the former. However, the detail of the numerical procedures is not referred here.

1.3. Function of detached breakwaters in the control of longshore currents

With the normal wave incidence, a pair of circulation cells of wave-induced current is formed behind the breakwaters. Since analytical solutions to mean water surfaces (wave set-up and set-down) and longshore currents were set forth by Bowen (1969) and Longuet-Higgins (1970), much study on the time-averaged properties of water-particle motion has been conducted.

The basic equations for these fluid motions are derived by temporally and vertically averaging a continuity equation of mass flux and a N-S equation, and are expressed as follows:

$$\frac{\partial\eta}{\partial t}+\frac{\partial U(h+\eta)}{\partial x}+\frac{\partial V(h+\eta)}{\partial y}=0 \tag{5}$$

$$\left.\begin{aligned}\frac{\partial U}{\partial t}+U\frac{\partial U}{\partial x}+V\frac{\partial U}{\partial y}&=-g\frac{\partial\eta}{\partial x}-\frac{1}{(h+\eta)}\left[\left(\frac{\partial S_{xx}}{\partial x}+\frac{\partial S_{xy}}{\partial y}+\tau_x\right)-\left(\frac{\partial R_{xx}}{\partial x}+\frac{\partial R_{xy}}{\partial y}\right)\right]\\ \frac{\partial V}{\partial t}+U\frac{\partial V}{\partial x}+V\frac{\partial V}{\partial y}&=-g\frac{\partial\eta}{\partial x}-\frac{1}{(h+\eta)}\left[\left(\frac{\partial S_{yx}}{\partial x}+\frac{\partial S_{yy}}{\partial y}+\tau_y\right)-\left(\frac{\partial R_{yx}}{\partial x}+\frac{\partial R_{yy}}{\partial y}\right)\right]\end{aligned}\right\} \tag{6}$$

where U and V are the depth and time averaged velocities of wave-induced current in the x- and y-direction, respectively; τ_x and τ_y are the time averaged bottom shear stresses; R_{ij},{(i,j)=(x,y)} is the depth and time averaged Reynolds' stress tensor; η is the mean water level and S_{ij},{(i,j)=(x,y)} is the radiation stress tensor introduced by Longuet-Higgins (1970); and h is the depth in still water.

Using linear wave theory, S_{ij} is expressed as follows:

$$\left.\begin{aligned}S_{xx}&=\frac{\rho g}{16}H^2\left[\frac{2C_g}{C}(\cos^2\theta+1)-1\right]\\ S_{xy}&=S_{yx}=\frac{\rho g}{16}H^2\sin 2\theta\\ S_{yy}&=\frac{\rho g}{16}H^2\left[\frac{2C_g}{C}(\sin^2\theta+1)-1\right]\end{aligned}\right\} \tag{7}$$

where ρ is the density of water, C and C_g are the celerity of wave propagation and group velocity, respectively, and θ is the angle of wave incidence.

The time averaged bottom shear stresses τ_x and τ_y are usually evaluated from the approximate expression using friction factor, the water particle velocity caused by waves at the bottom, and the velocity of wave-induced current.

The Reynolds' stress term is generally evaluated using a gradient-diffusion type expression with the eddy viscosity (ε) and is referred to as "lateral mixing term". Some heuristic models for eddy viscosity in an uniform longshore current on a long straight beach have been proposed. They are summarized in Table-2.

Table-2 Model for eddy viscosity in uniform longshore current on a long straight beach

	Lateral mixing term	Lateral mixing coefficient	Remarks
Bowen (1969)	$R_{xy} = \varepsilon \frac{d^2V}{dx^2}$	ε: constant	
Longuet-Higgins (1970)	$R_{yx}\rho h = \frac{d}{dx}\left(\rho \varepsilon h \frac{dV}{dx}\right)$	$\varepsilon = Nx\sqrt{gh}$	$0 < N < 0.016$ x: offshore distance from the shoreline
Thornton (1970)	$R_{yx} = \frac{d}{dx}\left(\varepsilon \frac{dV}{dx}\right)$	$\varepsilon = \frac{H^2}{8\pi^2} \frac{gT}{h} \cos^2\theta$	q: wave direction
James (1974)	$R_{yx}\rho h = \frac{d}{dx}\left(\rho h \varepsilon \frac{dV}{dx}\right)$	$\varepsilon =$ $N\sqrt{gh}h/S \quad : h \le h_b$ $N\sqrt{gh}h_b^2/(hS) : h > h_b$	S: bottom slope
Jonsson et al. (1974)	$R_{yx}\rho h = \frac{d}{dx}\left(\rho h \varepsilon \frac{dV}{dx}\right)$	$\varepsilon = \frac{4}{T} a_b^2 \cos^2\theta$	a_b: excursion length of water particle
Battjes (1975)	$R_{yx}\rho h = \frac{d}{dx}\left(\rho h \varepsilon \frac{dV}{dx}\right)$	$\varepsilon = M\left(\frac{5\gamma^2}{16}\right)^{1/3} S^{4/3} x\sqrt{gh}$	M: constant $\gamma = H/(h+\eta)$
Kim et al. (1986)	$R_{yx} = \begin{cases} \varepsilon \frac{d^2V}{dx^2} & : h \le h_b \\ 0 & : h > h_b \end{cases}$	$\varepsilon = AF^{1/3}\gamma S' x\sqrt{gh}$ $F = 5.3 - 3.3\xi - 0.07/S$ $S' = (-0.413\xi + 0.98)S$	A: constant $\gamma = H/L\sqrt{S}$ $S \ge 1/60$

The author et al. conducted a series of experiments in a wave basin to investigate the function of breakwater length l and distance from the initial shoreline X_{off} in controlling longshore currents in cases where angle of wave incidence is 150°. The results show that:

1) When a breakwater with a length of less than two times the incident wave length is constructed within the breaker zone($X_{off}/X_b=0.57$, where X_b is the width of the breaker zone), the velocity of longshore current decreased to about 1/2 of that on a natural beach.

2) When the breakwater is constructed in a location where $X_{off}/X_b>0.86$, although shore-side waves decrease significantly, longshore currents on a natural beach are not affected by the breakwater just behind the breakwater. However, a small weak circulation forms in the downdrift side of the breakwater.

1.4. Function of submerged breakwaters with wide crown width in the control of waves

The powerful effects of detached breakwater on wave transformation, especially the effect of diffraction, greatly affects the surrounding coast. It has also been pointed out that the breakwaters reduce the exchange of sea water and detracts from the natural coastal view.

Recently, to cope with these problems, sections of detached breakwaters are being replaced by submerged breakwaters, which are often referred to as artificial reefs, in Japan. Figure 3 is a diagram of submerged breakwaters constructed on the Niigata coast facing the Japan Sea.

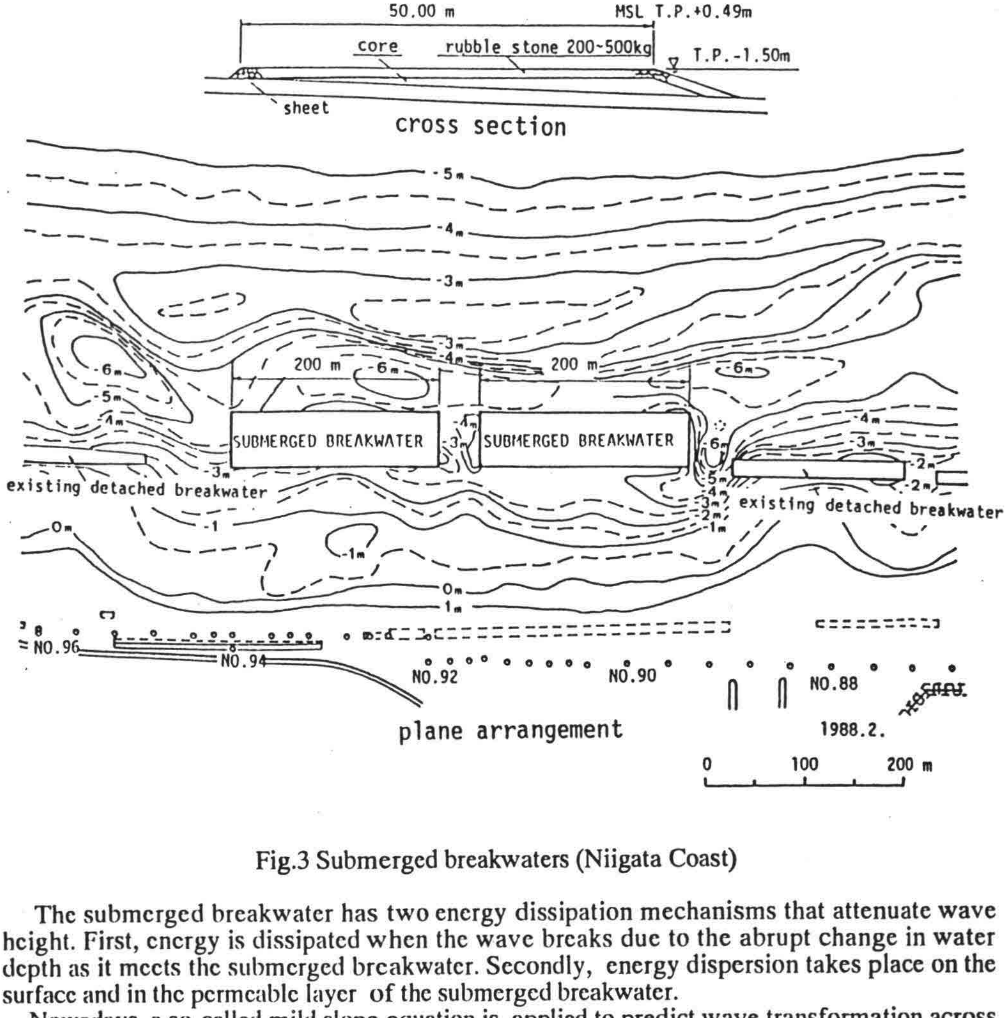

Fig.3 Submerged breakwaters (Niigata Coast)

The submerged breakwater has two energy dissipation mechanisms that attenuate wave height. First, energy is dissipated when the wave breaks due to the abrupt change in water depth as it meets the submerged breakwater. Secondly, energy dispersion takes place on the surface and in the permeable layer of the submerged breakwater.

Nowadays, a so-called mild slope equation is applied to predict wave transformation across submerged breakwaters (Mei,1978 and Yeang, 1982). However, the equation requires much CPU time. A procedure for predicting wave transformation over submerged breakwaters based on the conservation of wave energy is introduced here.

The equation for energy conservation on a permeable layer in a stationary state is expressed by

$$\frac{\partial}{\partial x}\{E(C_g\cos\theta + U)\} + \frac{\partial}{\partial y}\{E(C_g\sin\theta + V)\} + S_{xx}\frac{\partial U}{\partial x} + S_{xy}\left(\frac{\partial V}{\partial x} + \frac{\partial U}{\partial y}\right) + S_{yy}\frac{\partial V}{\partial y} = -D_{loss} \tag{8}$$

where E is the energy density of incident waves and D_{loss} is the total energy dispersion rate. D_{loss} is estimated as the sum of the energy losses in the permeable layer D_p and on the surface of the layer D_f and energy loss caused by wave breaking D_b.

The energy dispersion in the permeable layer D_p is expressed by

$$D_p = \frac{1}{T}\int_0^T (wp)_{z=-h}\, dt \tag{9}$$

where T is the wave period; w and p are the vertical water particle velocity and pressure at the surface of the permeable layer, respectively; and h is the depth on the permeable layer.

The energy dispersion rate per unit area on the permeable surface caused by boundary shear D_f is evaluated using the following expression for boundary shear stress τ on the bottom:

$$D_f = \frac{2}{T}\int_0^{T/2} \tau u_{z=-h}\, dt \tag{10}$$

According to linear wave theory, velocity potential on and in a permeable layer with permeability of K_p is given as follows (Deguchi et al., 1988):

on the permeable layer:

$$\phi = \frac{gH}{2\sigma}\mathrm{Re}\left[i\left\{\cosh\bar{k}z - \frac{1}{\bar{k}}\sinh\bar{k}z\right\}\exp\{i(\bar{k}x - \sigma t)\}\right] \tag{11}$$

in the permeable layer:

$$\phi_d = \frac{gH}{2\sigma}\mathrm{Re}\Big[\Big\{\frac{-i}{i+\gamma s}\cosh\bar{k}(h+z)(\cosh\bar{k}h + \frac{1}{\bar{k}}\sinh\bar{k}h)$$

$$-\frac{1}{\gamma}\sinh\bar{k}(h+z)\,(\sinh\bar{k}h + \frac{1}{\bar{k}}\cosh\bar{k}h\Big\}\exp\{i(\bar{k}x - \sigma t)\}\Big] \tag{12}$$

$$s = \{(1-\lambda)C_m + 1\}/\lambda$$

where λ, k_p, d are the void ratio, permeability and the thickness of the permeable layer, respectively; h is the depth on the permeable layer; σ is the angular frequency($=2\pi/T$); C_m is the added mass coefficient; $i^2 = -1$; and Re[ ] indicates the real part of the quantity in the brackets [ ]. The expression γ is the nondimensional permeability defined by the kinematic viscosity ν, K_p and σ in the form of $\gamma = k_p\sigma/\nu$. The expression of $\bar{k}$ is the complex wave number ($=\alpha+i\beta$), which satisfies the following dispersion relation on the permeable layer.

$$\sigma^2 = g\bar{k}\,\frac{(\gamma s+i)\sinh\bar{k}h\cosh\bar{k}d + \gamma\cosh\bar{k}h\sinh\bar{k}d}{(\gamma s+i)\cosh\bar{k}h\cosh\bar{k}d + \gamma\sinh\bar{k}h\sinh\bar{k}d} \tag{13}$$

The values of w and p in the permeable layer are expressed using ϕ_d as follows:

$$w = \gamma\frac{\partial\phi_d}{\partial z} \tag{14}$$

$$\frac{p}{\rho} = -s\frac{\partial\phi_d}{\partial t} - \frac{\nu}{k_p}\phi_d \tag{15}$$

From these relations, Eq.(9) is expressed as

$$D_f = \frac{\rho g}{4}H^2\beta \tag{16}$$

where β is the imaginary part of the complex wave number k which indicates the attenuation rate of wave height on the permeable layer. Figure 4 illustrates the relation between β and σ^2h/g when $\sigma^2H/g=0.1$, $k_p\sigma/\nu=0.5$ and $d/(h+d)=0.5$ (Deguchi et al., 1988).

To evaluate the value of D_f, Jonsson's expression for the bottom shear stress (Jonsson, 1978) was utilized.

$$\tau = \rho f u_{z=-h}^2 / 2$$

Jonsson (1978) and Riedel et al. (1972) have provided empirical expressions for friction factor f. When linear wave theory is used to evaluate the horizontal water particle velocity at a depth

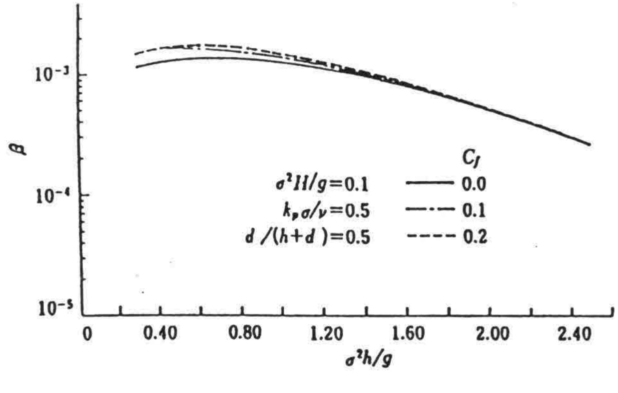

Fig.4 Relation between wave attenuation ratio β and σ^2h/g

of z=-h, D_f is expressed as follows:

$$D_f = \frac{2}{3}\pi^2 \rho f \left(\frac{H}{T\sinh kh}\right)^3 \tag{17}$$

where k is the usual real wave number at the depth of h.

On the other hand, various rates for energy dispersion after wave breaking have been proposed. In estimating the value of D_b, the existing dispersion rate proposed by Sawaragi et al. (1984) was used, where

$$D_b = 0.18\, F\rho^{-1/2}(h+\eta)^{-3/2}\, \cancel{E^{3/2}} \rightarrow \xi \tag{18}$$

$$F = \begin{cases} 5.3 - 3.3g - 0.07/S & : \text{inside the breaker zone} \\ 0 & : \text{outside the breaker zone} \end{cases}$$

where S is the bottom slope.

Figure 5 shows a comparison between the calculated wave heights and measured wave heights in a two-dimensional experiments on the submerged breakwater shown in Fig.2 (Sawaragi et al., 1989). Figures (a) and (b) correspond to non-breaking and breaking conditions on the breakwater, respectively.

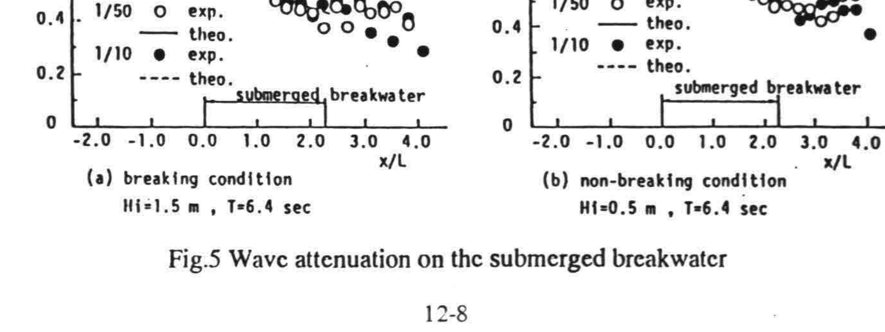

Fig.5 Wave attenuation on the submerged breakwater

1.5. Function of submerged breakwater in the control of nearshore currents

Wave-induced current around the submerged breakwater can be calculated using Eqs.(5) and (6) in a similar manner as for currents on the shore-side of the detached breakwaters.

Uda et al. (1988) conducted experiments on wave-induced flow patterns around a submerged breakwater with length l, opening width l', and distance from the shoreline X_{off}. The flow was classified into four patterns, as shown in Fig.6.

The flow patterns occurred under the following conditions:

Pattern I (Fig.(a)) : $l/X_{off} = 1$ to 4 and $l/l' < 4$,
Pattern II (Fig.(b)) : $l/X_{off} > 4$ and $l/l' < 4$,
Pattern III(Fig.(c)) : $l/X_{off} \approx 1$ and $l/l' < 4$,
Pattern IV (Fig.(d)) : $l/X_{off} = 1$ to 3 and $l/l' > 4$.

Based on these results, Uda et al. recommended that:

1) If the region in the shore-side of the submerged breakwater is to be used as a swimming area, or when uniform wave decay behind the breakwater is desired, the width of the opening l' must be less than $l/4$.
2) When there is likely to be a deposition of sediment on the shore-side of the breakwater, the value of l' should be greater than $l/4$ and the length of the breakwater l should be less than $4X_{off}$.

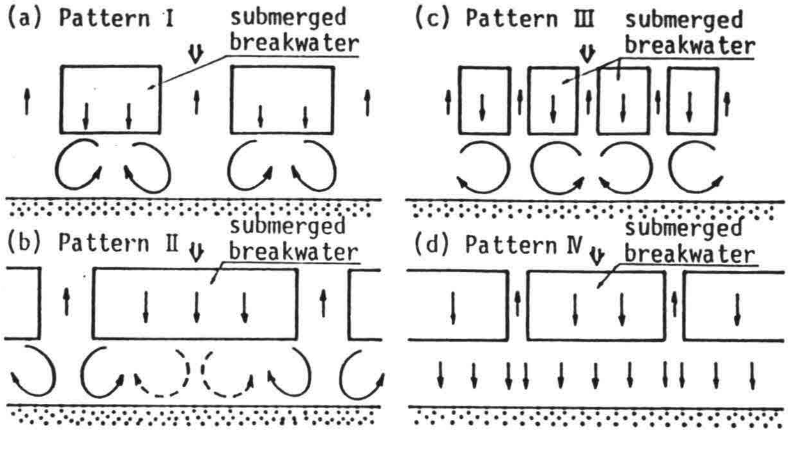

Fig.6 Patterns of wave-induced current around submerged breakwaters

2. FUNCTION OF DETACHED BREAKWATER IN THE CONTROL OF SEDIMENT MOVEMENT

2.1. Mechanism of formation of salient behind detached breakwater

Salients or a tombolos formed on the shore-side of the detached breakwaters are brought about by nonuniform longshore sediment transport on the shore-side of the breakwater. The topographic change caused by sediment transport in the littoral zone is expressed by the following equation:

$$\frac{\partial h}{\partial t} = \frac{1}{1-\lambda}\left(\frac{\partial q_x}{\partial x} + \frac{\partial q_y}{\partial y}\right) \tag{19}$$

where q_x and q_y are the local sediment transport rate in x(cross-shore) and y(longshore) directions, respectively; and h is the water depth measured downward from still water level.

We investigated the relation between the longshore sediment transport and topographic change by integrating Eq.(19) in the region where the sediment transport takes place. X_0 and X_{cr} were given the landward and the seaward limit of the significant sediment transport, respectively. The integration of Eq.(19) between $X=X_0$ and X_{cr} yields the following relation because the longshore and cross-shore sediment transport at $x=X_0$ and $x=X_{cr}$ are zero:

$$\frac{\partial}{\partial t}\int_{X_{cr}}^{X_0} h dx - h_{x=X_{cr}}\frac{\partial X_{cr}}{\partial t} + h_{x=X_0}\frac{\partial X_0}{\partial t} = \frac{1}{1-\lambda}\left(\frac{\partial}{\partial y}\int_{X_{cr}}^{X_0} q_y dx\right) \tag{20}$$

Change in a sectional area below a reference level along the x-axis A and a total longshore sediment transport rate Q_y is defined as follows:

$$A = \int_{X_0}^{X_{cr}} h dx \tag{21}$$

$$Q_y = \int_{X_0}^{X_{cr}} q_y dx \tag{22}$$

When the characteristics of the incident waves are constant, the second and the third terms in the left hand side of Eq.(20) approach zero. Under such conditions, Eq.(20) is written as follows:

$$\frac{\partial A}{\partial t} = \frac{1}{1-\lambda}\frac{\partial Q_y}{\partial y} \tag{23}$$

Furthermore, when the change in sectional area ΔA is expressed as the product of representative depth of topographic change $\bar{h}$ and shift in the shoreline Δl_s, Eq.(23) becomes

$$\frac{\partial l_s}{\partial t} = -\frac{1}{1-\lambda}\frac{1}{\bar{h}}\frac{\partial Q_y}{\partial y} \tag{24}$$

where l_s is measured positive landward.

Eq.(24) implies that the longshore gradient of total longshore sediment transport rate causes the change in shoreline contour. For example, the shoreline retreats if $\partial Q_y/\partial y > 0$ and the shoreline advances if $\partial Q_y/\partial y < 0$.

Figure 7 schematically illustrates wave patterns and changes in a shoreline. Oblique incident waves are diffracted by a detached breakwater which breaks the uniformity of longshore sediment transport. As a result, the shoreline is transformed according to the broken line in the figure.

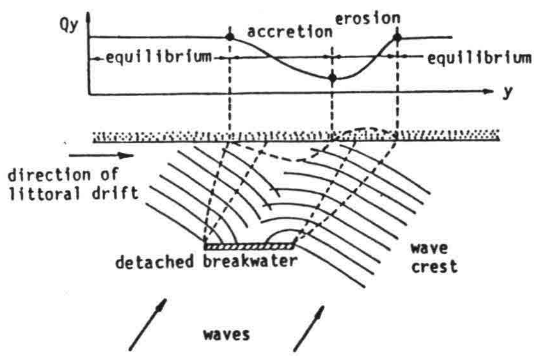

Fig.7 Schematic illustration of shoreline change on the shore-side of a detached breakwater.

2.2. Function of detached breakwater in the trapping of sediment

In designing detached breakwaters, the location, length and opening width must first be determined. Topographical changes on the shore-side of the breakwaters resulting from sediment trapped by breakwaters closely related to these values. Numerical simulation procedures which will be mentioned later can be of great help in the determination of these values.

First, the simplified relation between these values and the topographical changes are examined through field data. The Ministry of Construction of Japan studied the correlation between geometries of detached breakwaters and the topography on the shore-side of these breakwaters through field surveys (National Association of Sea Coast, 1978). A definition sketch of the geometry of detached breakwaters is shown in Fig.2. The expression X_{off} is the distance between the initial shoreline and the breakwater, l is the length of the breakwater, l' is the width of the opening, and T_x and T_y are the length and the width of the salient, respectively.

Figure 8 shows the relation between the geometry of the breakwater and a representative profile of the corresponding beach topography which is defined as the ratio between the area of the shore-side coast of the breakwater and the area of salient A_s:

$$A_s = \frac{\text{Area of saliant}}{\text{Area of the shore-side coast of the breakwater}} = \frac{T_x T_y/2}{X_{off}\, l} \tag{25}$$

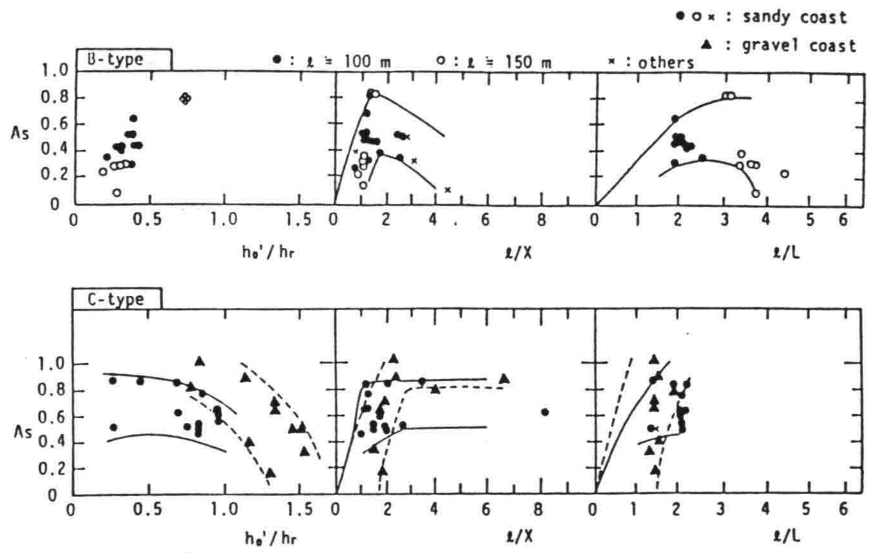

Fig.8 Topographic change on the shore-side of the detached breakwater as a function of location and length of detached breakwater

In Fig.8, h_0 is the water depth at the breakwater and, h_r and L are defined using the averaged wave height and period for the five largest incident significant waves during the year $[H_s]_5$ and period $[T_s]_5$ as follows:

$$h_r = [H_s]_5 \ ; \ L = \sqrt{g h_0}\, [T_s]_5.$$

B- and C-type coasts in the figure correspond to bar type coasts with gentle slopes and plane coasts with steep slopes, respectively. The values of l/l' for the large part of breakwater in Japan range between 0.3 to 0.5.

2.3. Numerical simulation for trapping of sediment by breakwaters

Sediment movement in the shore-side of the detached breakwater depends on both waves and currents. Given the wave and current fields in the shore-side of the breakwater, the rate of sediment transport there can be estimated using proper sediment transport formulas.

A number of formulas for predicting rate of sediment transport have been proposed by many investigators based on various sediment transport models. Those models are generally classified into two categories. One is the power model, originally proposed by Bagnold (1965) (for example, Komar, 1970; Walton et al., 1979; Watanabe et al.,1982).

The other is the flux model in which the rate of sediment transport is expressed as the product of sediment concentration and its migration speed (for example, Kana,1976; Tsuchiya et al., 1978; Sawaragi et al., 1986). There is a third group of formulas based on the rate of sediment transport in a unidirectional flow (for example, Iwagaki et al., 1962; Bijker, 1968).

Here, the following formulas for bed load transport rate(q_b) and suspended load transport rate(q_s) derived by the authors(Sawaragi et al., 1990) are used to examine the effects of detached breakwaters on longshore sediment transport rate:

$$q_b = 47\pi\sigma d_{50}^2(\psi_m-\psi_c)^{3/2}(\mathbf{U}/u_b) \tag{26}$$

$$\begin{aligned} q_s &= \int C\mathbf{U}\ dz \\ &= \left.\begin{aligned} &C_0\ (\varepsilon_{sz}/w_f)\ \mathbf{U} && : \text{outside the breaker zone} \\ &C_0\ \mathit{min}\ \{\varepsilon_{sz}/w_f, D\}\mathbf{U} && : \text{inside the breaker zone} \end{aligned}\right\} \end{aligned} \tag{27}$$

where d_{50} is mean grain size of bed material, ψ_c is the critical Shields' Number, **U** is the velocity vector of mean current, u_b is maximum water particle velocity at the bottom due to waves, C_0 is the concentration of sediment at the reference level, ε_{sz} is the diffusion coefficient of suspended sediment, w_f is the settling velocity of sediment, D is the total local depth, and $min\{\ ,\ \}$ indicates the minimum value of the two quantities in $\{\ ,\ \}$. The values for ψ_m, ε_{sz}/w_f and C_0 are related to the sediment and fluid properties as follows:

$$\psi_m = (f/2)|F_b|^2 / \{(\sigma_s/\sigma - 1)gd_{50}\} \tag{28}$$

$$\varepsilon_{sz}/w_f = 0.021exp\{0.5(f|F_b|^2/2)^{1/2}\} \quad \text{(in cgs unit)} \tag{29}$$

where $|F_b|$ is the water particle velocity due to waves and currents and is expressed as:

$$|F_b|^2 = \{u_b^2 + (2/\pi)u_b(Ucos\theta + Vsin\theta) + (U^2 + V^2)/4\} \tag{30}$$

$$C_0 = 0.347\ [0.688u_b / \{1.13(\sigma_s/\sigma-1)gw_fT^{1.77}\}] \tag{31}$$

Figure 9 compares the calculated and measured total longshore sediment transport rates Q_{yf} and Q_{ye} on the shore-side of the detached breakwater(Sawaragi et al.,1990) . The value of Q_{yf} is calculated by integrating local longshore sediment transport rate q_{by} and q_{sy} obtained from Eqs.(26) and (27). The velocity of wave-induced currents and that of water particles at the bottom are calculated by solving mild slope equations and the fundamental equations for wave-induced current.

The value of Q_{ye} is estimated from topographical change $\Delta h(x,y)$, measured over time interval Δt during the movable bed experiments:

$$Q_{ye}(y+\Delta y) = Q_{ye}(y) + \Delta A(y)\frac{\Delta y}{\Delta t}(1-\lambda) \tag{32}$$

$$\Delta A(y) = \int \Delta h(x,y)\ dx$$

where Δy is the interval of the measuring line.

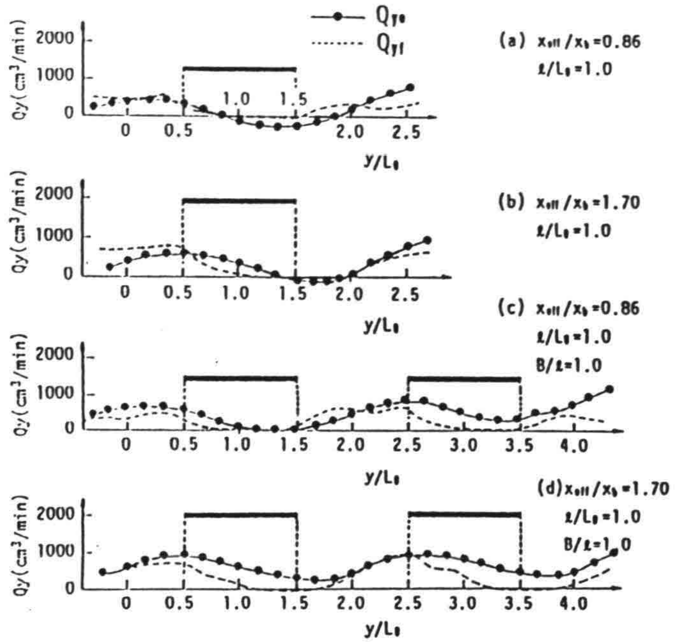

Fig.9 Distribution of longshore sediment transport rate on the shore-side of detached breakwaters

2.4. Topographical change on the shore-side of submerged breakwater

The effects of submerged breakwaters with wide crown width mentioned in the sections (1.4 and 1.5) on topographical change were examined using field data from a location on the Niigata Coast. The plane arrangement of the breakwater is shown in Fig.3. Figure 10 shows the annual change in the contour of the shoreline from 1986 (before the construction of the break-water) to 1988 (after the completion of two breakwaters) (Japan Inst. of Construction Eng., 1989).

The two submerged breakwaters were constructed in the gap between the detached breakwaters where the facing shoreline was subject to erosion. The shoreline facing the submerged breakwater indicates a quite different change compared with the shoreline facing the detached breakwaters. The latter advanced seaward, resulting in a salient. On the other hand, the shoreline facing the submerged breakwaters did not significantly advance seaward showed no marks of erosion. The shoreline configuration is also smooth compared to that facing the detached breakwaters. This indicates that well-designed submerged breakwaters have a mild but steady effect in maintaining shorelines.

3. STABILITY OF DETACHED BREAKWATERS

Detached breakwaters are usually constructed from rubble or wave absorbing blocks of various kinds. The stable weight of the rubble stone is usually determined by the so-called Hudson's formula. However, as pointed out by many researchers, the incident wave period is not taken into account in the formula. Consequently, some modifications in Hudson's formula have been proposed in which the significant wave height and period are used to express the

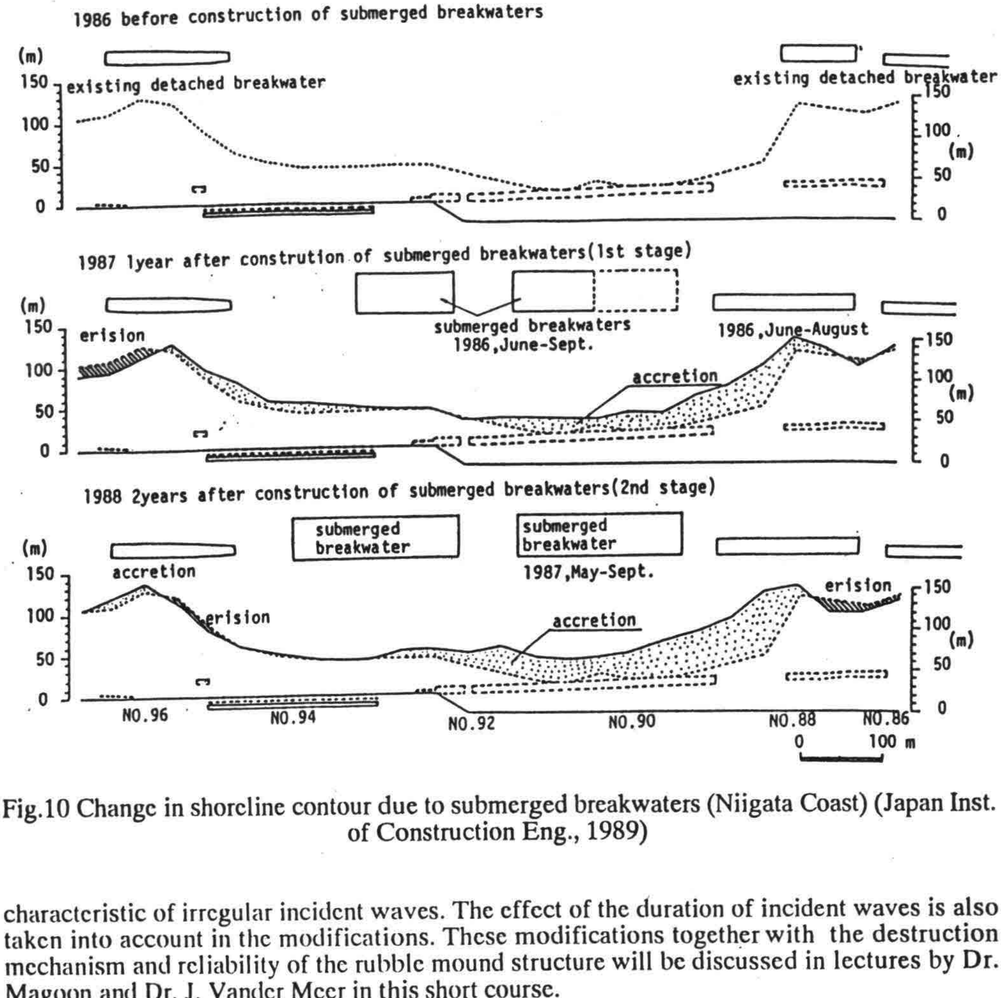

Fig.10 Change in shoreline contour due to submerged breakwaters (Niigata Coast) (Japan Inst. of Construction Eng., 1989)

characteristic of irregular incident waves. The effect of the duration of incident waves is also taken into account in the modifications. These modifications together with the destruction mechanism and reliability of the rubble mound structure will be discussed in lectures by Dr. Magoon and Dr. J. Vander Meer in this short course.

The author et al. also conducted a series of experiments on the destruction mechanism of rubble mound breakwaters by irregular waves and found that the destruction rate of a rubble mound breakwater depends largely on the run of the incident waves. The run of irregular incident waves is closely related to the peakedness of the frequency spectrum of incident waves. From these data, the author et al. derived a design procedure to directly determine the stable weight of rubble stone from the frequency spectrum. The design procedure is outlined below.

3.1. Effect of incident wave irregularity and grouping on the stability of rubble mound breakwater

The destruction rate of a rubble mound D_a' is usually determined by the number of rubble stones which are moved from their former place per total number of stones in the reference section, as follows:

$$D_a'(\%) = \frac{\text{number of stones moved from their former position}}{\text{total number of stones in the reference section}} \times 100 \tag{33}$$

To express the degree of destruction more accurately, the author et al. (1985) proposed a new definition for destruction rate D_a:

$$D_a(\%) = \frac{A_0'}{A_0} \times 100 \tag{34}$$

where A_0' is the destroyed volume of the cover layer (revetment) and A_0 is the destroyed volume of the cover layer when the destruction reaches the core layer as shown in Fig.11.

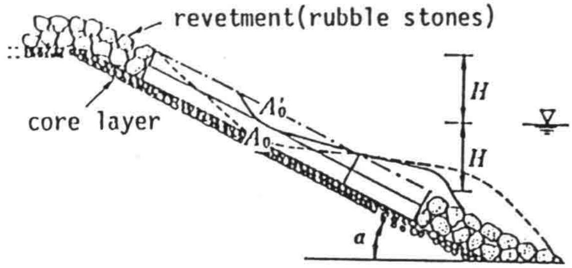

Fig.11 Definition sketch of damaged profile of rubble mound

The value of D_a is roughly related to D_a' by

$$D_a' = 0.2D_a. \tag{35}$$

Per Bruun (1979) pointed out that resonance on the slope of the breakwater strongly affects its stability. The author et al. (1983) found that resonance took place when the surf similarity parameter ξ is in the region of $2< \xi <3$.

Moreover, it is natural to consider that the run of high waves affect the destruction of rubble mound. Therefore, in the design of rubble mound breakwaters, the probability of the occurrence of both high waves and the surf similarity parameter of zero-up or zero-down cross waves have to be considered in determining the stable weight of the rubble stone.

The author et al. represented this probability using the conditional run length $j(\xi_o{}^*|_{H_s})$ which express the run length of $\xi_o{}^* = \xi/\xi_o = 2$ under the condition of $H \geq H_s$, where ξ_o is the surf similarity parameter of the maximum wave and H_s is the significant wave height. Furthermore, wave energy directly relating to the stability of the rubble mound breakwater is represented by the average of the energy sum of each wave in each of the runs derived above over each run length, defined by

$$E_{sum} = \frac{1}{8}\sum_{i=1}^{\infty} \rho g H_i^2 \ / \sum_{j=1}^{N} N_j \tag{36}$$

where N_j is the number of the run whose length is j, and H_i is the wave height of i-th wave in the run. The author et al. obtained the following relation between E_{sum} and the mean run length $j(\xi_o{}^*|_{H_s})$:

$$\frac{E_{sum}}{\rho g H_s^2/8} = 0.78j(\xi_o{}^*|_{H_s}) - 0.44 \tag{37}$$

The destruction rate D_a of a uniform slope breakwater is related to E_{sum} by

$$D_a = 153.8\left[\frac{E_{sum}}{\rho_s g l_a^2}\ \frac{\tan\alpha}{\tan\psi}\right] - 30.1 \tag{38}$$

where ρ_s is the density of the rubble stone, l_a is the representative diameter of the rubble stone, ψ is the friction angle of the rubble stones, and $\tan\alpha$ is the slope of the breakwater.

The mean run length $j(\xi_0^*|_{H_s})$ defined above is closely related to the peakedness of the frequency spectrum of incident waves Q_p by the following relation:

$$j(\xi_0^*|_{H_s}) = 3Q_p/16 + 0.81 \quad (39)$$

where E(f) is the frequency spectrum of incident waves,

$$Q_p = \frac{2}{m_0}\int_0^\infty f\ E(f)\ df \quad (40)$$

Assuming that the weight of the rubble stone W is expressed by $W = \rho_s g l_a^3$, the stable weight of rubble on the uniformly sloping mound is determined from Eqs.(37) to (39) as follows:

$$W = \left[\frac{\rho g(6.15Q_p+20.0)}{(\rho_s g)^{1/3}(D_a+30.1)}\ \frac{\tan\alpha}{\tan\psi}\right]^{3/2} \cdot H_s^3 \ \text{: for uniform slope} \quad (41)$$

When the rubble mound breakwater of uniform slope is damaged, the slope of breakwater deforms into a composite shape as shown by a thick solid line in Fig.12.

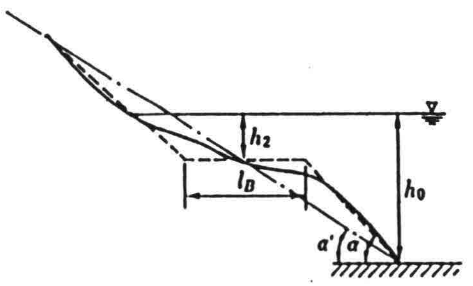

Fig.12 Definition sketch of rubble mound breakwater of composite slope

If the original slope of the rubble mound breakwater is a composite shape as shown by the dotted line in Fig.12, the breakwater will be more stable and the weight of rubble needed can be reduced. The author et al. carried out experiments on the stability of a rubble-mound breakwater of composite slope whose hypothetical slope $\tan\alpha'$ is 1/2.3 and obtained the following relation for determining the stable weight for the rubble stone:

$$W = \left[\frac{\rho g(5.46Q_p+17.73)}{(\rho_s g)^{1/3}(D_a+36.3)}\ \frac{\tan\alpha'}{\tan\psi}\right]^{3/2} H_s^3 \ \text{: for composite slope} \quad (42)$$

Figure 13 illustrates the relation between the value of Q_p and the stable weight of the rubble stone W. It can be seen that the stable weight W increases in proportion to Q_p.

Comparing the results for the cases with different values of l_B, the stability becomes higher with increasing l_B. As to the influence of h_2 on the stability, the experiments with $h_2/h_0 = 1/4$ show better results than those with $h_2/h_0 = 1/2$. The reason for this is considered that the hydrodynamic forces become less impulsive and the resonance on the slope occurs less frequently, with h_2 decreasing. The quantitative estimation of the influence of l_B and h_2 must be studied further.

Figure 14 shows the relation obtained between the stable weight of the rubble stone W and destruction rate D_a when Q_p=2.5 and H_s=7m.

In the figure, the stable weight of the rubble stone calculated from Hudson's formula is also shown. The calculated weight from Eq.(41) with an allowable destruction rate (D_a) of 20% seems to correspond to that evaluated by Hudson's formula. The determination of allowable destruction rate is a practical problem for future study.

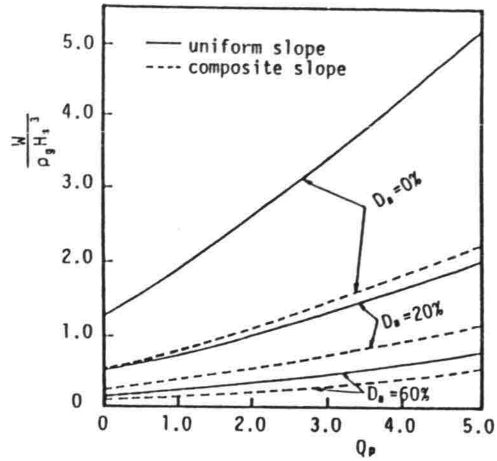

Fig.13 Stable weight of rubble stone as a function of Q_p

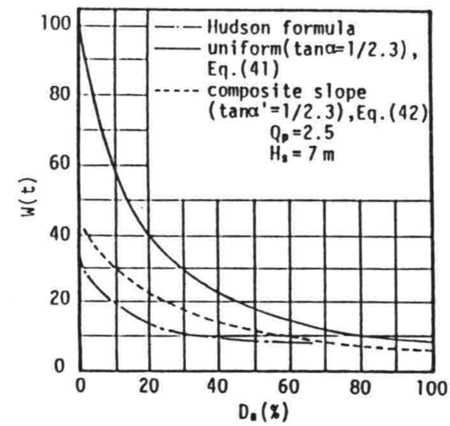

Fig.14 Relation between stable weight of rubble stone and destruction rate

Stable weight for composite type breakwaters is approximately 1/2 that for uniform slope breakwaters, given the same rate of destruction; in other words, smaller materials can be used in constructing rubble-mound breakwaters of composite slope.

3.2. Stable weight of rubble stones for submerged breakwaters

The Public Research Institute of the Ministry of Construction of Japan (Uda,1988) conducted a series of experiments to determine the stable weight of rubble stones for submerged breakwaters before starting construction of the submerged breakwaters on the Niigata coast shown above in Fig.3. They found that rubble stones on the submerged breakwater were first lifted up by the lift force and then moved from the surface of the breakwater. From the experiment, the following formula for determining stable weight was proposed, based on the balance between the weight of the stones and the lift force acting on them, in the cases where $H_o'/h>0.3$:

$$W_s = \left(S_n \frac{f_u}{(\rho_s/\rho-1)\ cos\ \alpha}\right)^3 \rho_s K_v R^3 \tag{43}$$

in which

$S_n = C_L K_a/2K_v$ (Stability Number)

$$f_u = \frac{u_{max}}{\sqrt{gR}} = 8\,exp\left(-1.5\frac{H_o'}{h_o} - 2.8\frac{R}{H_o'}\right) + 0.2$$

$K_v = V_r/d^3$, $K_a = A_r/d^2$

where C_L is the lift force coefficient, V_r and A_r are the volume and sectional area of the rubble stone, H_0' is the equivalent deep water wave height of incident waves, h_0 is the depth of the sea floor at the submerged breakwater and R is the depth at the crown of the breakwater. The values of S_n and K_v depend on the material used for rubble. The following values are given by the Ministry of Construction of Japan:

$S_n = 0.9$, $K_v = 0.5$: natural stone
$S_n = 0.9$, $K_v = 0.5$ to 1.0 : wave absorbing block

4. CONCLUSIONS

The functions of detached breakwaters and submerged breakwaters in controlling waves, wave-induced currents and sediment movement were discussed. As has already been reported by many researchers, detached breakwaters are very effective in controlling incident waves and salient or tombolo formation due to deposition of sediment sometime result in sever erosion of downstream coasts.

On the other hand, submerged breakwaters have a relatively mild but steady effect in retaining shore-side sediment and have little effect on the surrounding coasts. Therefore, submerged breakwaters are recently replacing detached breakwaters in Japan. However, there are some issues related to submerged breakwaters: 1)They may become fatal obstacles for fishing boats or small pleasure boats; 2)The effect of a submerged breakwater on a coast with a wide tidal range is not obvious because the hydraulic function of the submerged breakwater depends on the water depth at the crown.

In determining the stable weight of rubble stones for a submerged breakwater, it is important to consider the effects of irregularity and grouping of incident waves. Naturally, the wave period should also be taken into consideration, as was pointed out by Bruun and the author. From this point of view, the formula for determining the stable weight of rubble for submerged breakwaters as proposed by the Ministry of Construction of Japan needs to be further studied.

SYMBOLS

A	Change in sectional area below a reference lovel along x-axis
A_r	Sectional area of rubble stone
A_s	Areal ratio of salient and shore-side coast of breakwater
A_o	Destroyed volume of rubble mound breakwater when the destruction reaches the core layer
A_o'	Destroyed volume of cover layer of rubble mound breakwater
a_b	Excurtion length of water particle
B	Breakwater width at still water level
C	Celerity, Suspenced sediment concentration
C_g	Group velocity
C_L	Lift force coefficient

C_m Added mass coefficient
C_o Reference concentration
D_a Destructionratcofrubble mound breakawter determinedfromthe volume of deformed slope
D_a' Destruction rate of rubble mound breakwater determined from the number of rubble stones moved from their original place
D_b Energy loss due to breaking waves
D_f Energy loss caused by boundary shear
D_{loss} Total energy loss
D_p Energy loss took place in permeable layer
d Thickness of permeable layer
d_{50} Mean grain size
E Energy density of incident waves
F_b Water particle velocity caused by waves and currents
E(f) Frequency spectrum of incident waves
E_{sum} Wave energy directly relatingtothe stabilityofrubble mound breakwater
f Friction factor
g Gravity accerelation
H_i Incident wave height
H_s Significant wave height
$[H_s]_5$ Average of five largest incident significant wave heights
H_o' Equivalent deep water wave height
h Depth in still water
$\bar{h}$ Representative depth of topographic change
h_b Water depth at breaking point
h_o Water depth at the foot of breakwater
h_r Representative depth
h_s Crown height from still water level
h_2 Berm depth of rubble mound breakwater of composite slope
k Wave number
$\bar{k}$ Complex Wave number on permeable layer
K_a Coeffisient relating shape of rubble stone
K_g Diffraction coefficient
k_p Permeability
K_t Transmission coefficient
K_v Coefficient relating shape of rubble stone
L Wave length
l Length of detachewd breakwater
l' Length of opening in the row of detached breakwaters
l_a Representative diameter of rubble stone
l_B Berm width of rubble mound breakwater of composite slope
m_o 0-th moment of frequency spectrum
p Pressure
Q_p Peakedness of frequency spectrum
Q_y Total longshore sediment transport rate
Q_{ye} Total longshore sediment trasnport rate estimated from toporgaphic change
Q_{yf} Total longshore sediment transport rate calculated from flux model
q_b Local bed load transport rate
q_s Local suspended sediment trnasport rate
q_i Local sediment transport rate
R Depth at the crown of submerged breakwater
$R_{i,j}$ Depth and time averaged Reynolds' stress tensors
S Bottom slope
$S_{i,j}$ Radiation stress tensors

S_n	Stability number for submerged breakwater
T	Wave period
$[T_s]_5$	Average of five largest significant wave periods
T_x	Length of salient
T_y	Width of salient
U	Time and vertically averaged velocity of wave induced current in x (offshore) direction
u_b	Maximum water particle velocity due to waves at bottom
u_{max}	Maximum water particle velocity at the wave crest
V	Time and vertically averaged velocity of wave-induced current in y (longshore) direction
V_r	Volume of rubble stone
W	Weight of rubble stone
w	Water particle velocity in vertical direction
w_f	Settling velocity
x	Offshore distance
X_b	Width of breaker zone
X_{off}	Distance between initial shoreline and breakwater
X_o	Landward limit of significant sediment transport
X_{cr}	Seaward limit of significant sediment transport
y	Longshore distance
z	Vertical distance
α	Slope of breakwater
α'	Hypothetical slope of rubble mound breakwate of composite slope
β	Imaginary part of complex wave number
ψ	Friction angle
ψ_c	Critical Shields' number
ψ_m	Shields' number
ε	Eddy viscosity
ε_{sz}	Diffusion coefficient of suspended sediment
ϕ	Velocity potential
ϕ_d	Velosity potential in permeable layer
ϕ_i	Velocity potential of incident waves
ϕ_s	Velocity potencial of scattered waves
λ	Void ratio
η	Displacement of mean water level
η_c	Hight of wave crest from the still water level
ν	Kinematic viscosity
γ	Ratio of wave height and total water depth or Nondimensional permeability ($=k\rho\sigma/\nu$)
ρ	Density of water
ρ_s	Density of rubble stone
θ	Angle of wave incidence
σ	Angular frequency
τ_i	Time averaged bottom shear stress
ξ	Surf simularity parameter

ξ_0 Surf similarity parameter of the maximum wave

ξ_0^* $= \xi/\xi_0$

REFERENCES

BAGNOLD, R.A. (1965). The flow of cohesionless grains in fluids, Proc. Roy.Soc. Series A.964, Vol.249, pp.235-297.

BATTJES, J.A. (1975) A note on modeling of turbulence in the surf zone, Proc. Symp. Modeling Technique, pp.1050-1061.

BIJKER, E.W. (1968). Littoral drift as a function of waves and current, Proc. 11st ICCE, pp.415-435.

BOWEN, A.J. (1969). The generation of longshore current on a plane beach, J. Marine Res., Vol.27, pp.206-215.

BRUUN, P. (1979). Common reasons for damage or breakdown of rubble mound breakwaters, Coastal Eng., Vol.2, pp.261-273.

DEGUCHI, I., T. SAWARAGI, and K. SHIRATANI (1988). Study on the applicability of nonlinear, unsteady Darcy Law to wave transformation on permeable layer, Proc. 35th Japanese Conf. Coastal Eng., JSCE, pp.478-491 (in Japanese).

IWAGAKI, Y. and T. SAWARAGI (1962). A new method for estimation of the rate of littoral sand drift, Coastal Eng. in Japan, Vol.5, pp.67-79.

JAMES, I.D. (1974). A nonlinear theory of longshore current, Estuarine and Coastal Marine Science, Vol.2, pp.207-234.

JAPAN INST. OF CONSTRUCTION ENG. (1989). Report of study on artificial reefs at Niigata Coast, Publ. Japan Institute of Construction Engineering, 28p. (in Japanese).

JONSSON, I.G., O.SKOVGAAD and T.S.JACOBSEN (1974). Computation of longshore currents, Proc.14th ICCE, pp.699-714.

JONSSON, G.I. (1978). A new approach to oscillatory rough turbulent boundary layers, Series Paper 17, Inst. of Hydrodynamics and Hydraulic Eng., Tech. Univ. of Denmark.

KANA, T.J. (1976). Sediment transport rates and littoral processes near Price Inlet, Terrigeneous clastic depositional environments, ed. by M.O, Hays and Kana, T.W., Univ. of South Carolina, pp.II-158-171.

KIM, K.H., T. SAWARAGI and I. DEGUCHI (1986). Lateral mixing and wave direction in the wave-current interaction region, Proc. 20th ICCE, pp.366-380.

KOMAR, P.D. and D.L. INMAN (1970). Longshore sand transport on beaches, J. Geophys. Res., Vol.75, pp.5914-5927.

LONGUET-HIGGINS, M.S. (1970). Longshore currents generated by obliquely incident sea waves, 1 and 2, J. Geophys. Res., Vol.75, pp.6778-6801.

MEI, C.C. (1978). Numerical methods in water wave diffraction and radiation, Ann. Rev., Fluid Mech., Vol.10, pp.393-416.

NATIONAL ASSOCIATION OF SEA COAST (1987). Technical standard for shore protection works in Japan, Published by National Association of Sea Coast, 269p (in Japanese).

NUMATA, J. (1975). Experimental studies on wave absorbing effect of rubble mound breakwater, Proc. 22nd Japanese Conf. on Coastal Eng., pp.501-506 (in Japanese).

PULLIN, D.L. and P.N. JOUBERT (1984). Behavior of converging-channel break water; Theory and experiment, J. Fluid Mech., Vol.141, pp.123-138.

RIEDEL, H.P., J.W. KAMPHUIS and A. BREBNER (1972). Measurements of bed shear stress under waves, Proc.13rd ICCE, pp.587-604.

RYU, C.R. and T. SAWARAGI (1985). A new design method of rubble mound break- water, Proc.20th, ICCE, pp.2188-2202.

SAWARAGI, T., C.R.RYU and K. IWATA (1983). Considerations of the destruction mechanism of rubble mound breakwaters due to resonance phenomena, Proc. 8th IHC, pp.3.197-3.208.

SAWARAGI, T., I. DEGUCHI and K.H. KIM (1984). Energy loss and wave set-up in the surf zone, Tech. Rept. of The Osaka Univ., Vol.34, No.1179, pp.329-338.

SAWARAGI,T. (1986). Recent study on the littoral sediment transport, Lecture note of 18th Seminar on Coastal Eng., National Assoc. of Sea Coast, pp.11-18 (in Japanese).

SAWARAGI, T., I. DEGUCHI and Y.OKAHARA (1989). Effects of submerged breakwater of wide crown width on controlling wave height and its scale effects, Proc. 36th Japanese Conf. Coastal Eng., pp.633-637 (in Japanese).

SAWARAGI, T., I. DEGUCHI and G. Y. KIM (1990). Function of detached breakwater to control longshore sediment transport, Proc.22nd ICCE, pp.2603-2615.

SPRING, B. H. and P.L. MONKMEYER (1975). Interaction of plane waves with a row of cylinder, Proc. Civil Eng. in the Oceans III, ASCE, Vol.3, pp. 979-998.

THORNTON, E.B. (1970). Variation of longshore current across the surf zone, Proc.12nd ICCE, pp.291-308.

TOYOSHIMA, O. (1986). Shore protection works, Lecture Notes on Practical Design of Coastal Structures, The ministry of Construction, Japan (in Japanese).

TSUCHIYA, Y. and T. YASUDA (1978). A mathematical model of beach change, Proc.25th Japanese Conf. on Coastal Eng.,pp.189-193 (in Japanese).

UDA, T. (1988). Function and design method of artificial reef, Tech.memo., Published by Work Research Institute, No.2696, Ministry of Construction, 79p., 1988 (in Japanese).

WALTON, J.L. and T.Y.CHIU (1979). Littoral sand transport on beaches, Rept. No.TR-041, Univ. of Florida, Gainsvill, 345p.

WATANABE, A. (1982). Numerical models of nearshore currents and beach deformation, Coastal Eng, In Japan, Vol.25, pp.147-161.

YEANG, R.W. (1982) Numerical methods in free surface flows, Ann. Rev. Fluid Mech., Vol.14, pp.395-442.